Int.J.Curr.Microbiol.App.Sci (2023) *12*(01): 171-189

International Journal of Current Microbiology and Applied Sciences
ISSN: 2319-7706 **Volume 12 Number 1 (2023)**
Journal homepage: http://www.ijcmas.com

Original Research Article https://doi.org/10.20546/ijcmas.2023.1201.020

Black Tea Extract Prevents iAs Induced Transformation of HaCaT Cells via Modulation of Cellular Damage, Inflammation and TGF-β Signalling Cascade

Archismaan Ghosh and Madhumita Roy*

Department of Environmental Carcinogenesis and Toxicology, Chittaranjan National Cancer Institute, 37, S P Mukherjee Road, Kolkata – 700026, India

**Corresponding author*

A B S T R A C T

Chronic exposure to inorganic arsenic (iAs) leads to development of cancer of various organs, most prevalent being skin cancer. iAs induces its carcinogenic potential by excess generation of free radicals, which induces DNA, protein, lipid damage; supresses activity of antioxidant enzymes; enhances prolonged inflammatory conditions and modulates TGF-β signalling cascade, all of which promote carcinogenesis. Black tea extract (BTE), a popular beverage and an established antioxidant, has been used in present study to combat the ill effects of iAs exposure. Present study has been conducted on normal human skin keratinocytes, HaCaT cells. Estimation of Reactive Oxygen Species (ROS) and Reactive Nitrogen Species (RNS) generation was done using 2',7'-dichlorodihydrofluorescein diacetate (DCFH-DA) and Greiss reagent. Damage to DNA (by Micronuclei and Comet assay), protein (by protein carbonyl assay kit) and lipid (by lipid peroxidation) were assessed. Activity of antioxidant enzymes, inflammatory cytokines, p50 and p65 subunits of NF-κB were assessed using respective kits. Immunoblotting assay was performed to assess expression of TGF-β and modulation of its downstream signalling molecules. Results indicate that BTE quenches iAs induced free radicals; inhibits DNA, protein and lipid damage; prevents deactivation of antioxidant enzymes; suppresses inflammation and prevents EMT inducing modulation of TGF-β pathway, thus thwarting iAs induced carcinogenesis in HaCaT cells.

Keywords

Inorganic Arsenic (iAs), Black tea Extract (BTE), ROS, RNS, TGF-β

Article Info

Received:
10 December 2022
Accepted:
28 December 2022
Available Online:
10 January 2023

Introduction

Colourless, odourless, tasteless metalloid Arsenic, 33rd element in the periodic table, is omnipresent in our surroundings (Roy *et al.*, 2014). In nature, it is found in both inorganic and organic forms, inorganic form of arsenic is considered to be more toxic than the organic form (Rahaman *et al.*, 2021). Arsenic is a major environmental pollutant and it may contaminate air, water and soil due to both natural and anthropogenic causes. Groundwater is one of the major sources of drinking water in the world and contamination of it by inorganic Arsenic (iAs) is a serious health hazard worldwide (Chung *et al.*, 2014). Humans chronically exposed to iAs develop numerous dermatological, cardiovascular, gastrointestinal as well as neurological diseases but most serious amongst them being cancer of different

organs. Chronic iAs exposure has been linked to development of skin, bladder, kidney, liver, lungs and prostate cancer (Chakraborti *et al.,* 2018). The preliminary manifestations of chronic iAs exposure appears on the skin in the form of spotted melanosis, hyperpigmentation, hypopigmentation etc. many of which progress into Bowen's disease (in-situ carcinoma) and invasive squamous cell carcinoma (SCC) of the skin (Hunt *et al.,* 2014).

One of the predominant ways in which iAs induces its carcinogenicity is, by induction of excess Reactive Oxygen Species (ROS) (Ghosh *et al.,* 2020). Chronic iAs exposure leads to increased ROS generation which further results in elevated DNA, protein and lipid damage (Ghosh *et al.,* 2021). ROS can induce modification of DNA bases resulting in the formation of 8-oxoguanine DNA adducts as well as induce DNA stand breaks (Srinivas *et al.,* 2019). It also promotes accumulation of DNA damage by inhibiting the activity of DNA repair enzymes. ROS promotes oxidation of amino acids which results in the formation of protein carbonyl. The extent of protein damage can be estimated by quantification of protein carbonyl formation (Sinha *et al.,* 2010). ROS can cause damage to cell membrane by promoting peroxidation of the polyunsaturated fatty acids, leading to formation of malondialdehyde (MDA), which is toxic for the cells. Quantification of the moles of MDA generated is used to assess the extent of lipid damage inflicted upon the cell membrane (Yusupov *et al.,* 2017). Chronic iAs exposure also leads to inhibition of activity of antioxidant enzymes like Superoxide Dismutase (SOD), Catalase, Glutathione peroxidase (GPX), Glutathione reductase (GR), Glutathione S-transferase (GST) etc., which further results in the accumulation of unquenched ROS (Ghosh *et al.,* 2021). Excess ROS generation has also been linked to inflammation (Mittal *et al.,* 2014) and chronic inflammation is an established hallmark of tumour progression (Hanahan and Weinberg, 2011). Chronic iAs exposure have been reported to induce secretion of pro-inflammatory cytokines TNF-α, IL-2, IL-6, IL-8, IL-13, IL-17a and IL-22 (Ghosh *et al.,* 2021). Upregulation of these cytokines have been implicated in various cancers. Studies have confirmed that, ROS can promote the upregulation and cytosolic translocation of NF-κB, the downstream effector molecule of inflammatory cytokines, which can modulate cell growth and proliferation (Lingappan, 2018). Therefore, promotion of chronic inflammatory conditions, may be one of the routes of iAs induced carcinogenesis.

Excess ROS generation can modulate many signalling pathways which control cell growth and proliferation, one such signalling pathway is the Transforming Growth Factor Beta (TGF-β) pathway. Modulation of the TGF-β pathway is implicated in many cancers and ROS seems to be an effective modulator of TGF-β (Krstić *et al.,* 2015). Elevated ROS is known to promote the secretion and activity of TGF-β and its downstream signalling molecules (Chung *et al.,* 2021). TGF-β is known to have a dual role in tumorigenesis, during initial stages of carcinogenesis, it prevents cell proliferation and promotes apoptosis but in later stages it promotes tumour development (Baba *et al.,* 2022). TGF-β transmits its downstream signalling, canonically, via the Suppressor of Mothers against Decapentaplegic (Smad) pathway (Clayton *et al.,* 2020). Smad 2/3 is known as Receptor regulated Smad (R-Smad) and they are activated by the phosphorylated cytosolic part of TGF-β receptor type 1. Phosphorylated R-Smads form a complex with the common mediator Smad (Smad 4) and are translocated to the nucleus, where they act as transcription factor and transcribe genes involved in cell growth, cell proliferation etc (Clayton *et al.,* 2020). TGF-β can also transmit its signalling noncanonically via the Phosphoinositide 3 Kinase (PI3K)-protein Kinase B (AKT) pathway and the Mitogen-activated protein kinase (MAPK) pathway (Zhang, 2009). Studies have linked upregulation of TGF-β with the induction of Epithelial to Mesenchymal transition (EMT) (Hao *et al.,* 2019). EMT is an important phenomenon in carcinogenesis, where cells lose their epithelial characteristics and acquire mesenchymal features which helps them to invade within the tissue and ultimately promote metastasis (Lamouille *et al.,* 2014). Therefore,

modulation of TGF-β by iAs induced ROS may promote EMT and hence carcinogenesis. According to a study, activation and upregulation of Smad 3 and Smad 4 was observed in TGF-β induced EMT, hinting at oncogenic role of the two signalling proteins (Vincent *et al.,* 2009) whereas another study exhibited contrasting results, where Smad 2 and Smad 3 exhibited tumour suppressor properties and loss of Smad 2 and Smad 3 was found to promote EMT and carcinogenesis (Rose *et al.,* 2018). Loss of Smad 4 have also been reported in SCC of the skin and few other cancers (Hernandez *et al.,* 2019). The signalling molecules of the non-canonical TGF-β pathway like PI3K, AKT, p38 and JNK have also been found to exhibit tumour promoting and EMT inducing role (Lu *et al.,* 2019; Kalli *et al.,* 2022; Zhan *et al.,* 2013). Upregulation of these proteins have been highly implicated in tumorigenesis. Therefore, to understand the role of TGF-β in iAs induced carcinogenesis, the modulation of downstream TGF-β signalling also needs to be studied. As most of the carcinogenic modulations brought about by chronic iAs exposure occurs mainly due to generation of excess ROS, therefore, quenching of ROS can be an excellent strategy to combat its carcinogenicity. Many phytochemicals, extracted from natural sources, have excellent free radical quenching ability, which may promote their use as an antioxidative and chemopreventive agent, with minimum or no side effects (Ranjan *et al.,* 2019). Black tea, which is the most popular beverage worldwide, has exhibited excellent antioxidative properties (Ghosh *et al.,* 2022a; Ghosh *et al.,* 2022b). The chemopreventive and antioxidative potential of Black tea Extract (BTE), which is the aqueous extract of processed tea leaves, has been assessed in the present study. The present study aims to assess the evil effects of chronic iAs exposure in HaCaT cells. Consequence of this may lead to generation of free radicals, resulting in DNA, lipid and protein damage. Therefore, we aim to quantitate the extent of damage caused to DNA, protein and lipid; to estimate the activity of pro-inflammatory and anti-inflammatory cytokines; to investigate expression of TGF-β and its down-stream signalling molecules upon chronic iAs exposure. Finally, we aim to look into the amelioration of the above-mentioned events by the administration of BTE, in HaCaT cells. The effect of chronic iAs exposure can often be seen on the skin of the exposed individuals, which may eventually develop into SCC. Therefore, the present study has been conducted on normal human skin keratinocytes HaCaT cells (Boukamp *et al.,* 1988). In order to mimic the condition of chronic iAs exposure, the HaCaT cells were continuously maintained in medium containing iAs. To assess the modulatory property of BTE, the cells were simultaneously exposed to iAs and BTE. The cells were closely monitored and experiments were performed at regular time intervals.

Materials and Methods

Fetal bovine serum (FBS), 1:1 mixture of Dulbecco's Modified Eagle Medium: Ham's Nutrient Mixture F-12 (DMEM/F-12), acrylamide, *N*, *N′* -methylenebis-acrylamide were obtained from Invitrogen BioServices India Pvt. Ltd. (Bangalore, India). Sodium arsenite (NaAsO2), bovine serum albumin (BSA) and MTT (3-(4,5-Dimethylthiazol-2-yl)-2,5-Diphenyltetrazolium Bromide) were bought from Sigma-Aldrich, USA. Goat IgG anti-rabbit and anti-mouse (alkaline phosphatase conjugated) were purchased from Genetex CA, (USA), BCIP-NBT (5-bromo-4-chloro-3- indolyl phosphate/nitro blue tetrazolium) was bought from Santa Cruz Biotechnology (California, USA); nitrocellulose membrane was purchased from, Amersham Biosciences (UK); Glycine, Tris and SDS (sodium dodecyl sulphate) was purchased from Amresco (Ohio, USA).

Preparation of black tea extract (BTE)

Black tea extract (BTE) was prepared by boiling 2.5 g of black tea in 100 ml of Milli-Q water resulting in 2.5% infusion. Lyophilisation was performed using a SCANVAC lyophilizer and the obtained powder was stored at 4°C. A grand stock solution of 100 µM BTE was obtained by reconstituting the lyophilized powder in Milli-Q water. The grand stock was added

in the medium of the cells so that the final concentration of the BTE solution was 1 µM.

Determination of safe dose of iAs and BTE using MTT assay

Non-toxic dose of iAs and BTE were determined via the MTT [3-(4,5-dimethythiazol-2-yl)-2,5-diphenyl tetrazolium bromide] assay, which was performed according to the protocol of (Ghosh *et al.,* 2022b). Logarithmic doses of iAs and BTE were administered to the cell and incubated for 48 hours. From the obtained results, a safe dose for iAs, 100 nM and that of BTE, 1 µM was selected, which was administered to the cells.

Cell culture and treatment

HaCaT cells were cultured in Dulbecco's Modified Eagle Medium: Ham's Nutrient Mixture F-12 (DMEM/F-12), mixed in 1:1 ratio, which was supplemented with 10 % of FBS and antibiotics (gentamycin, streptomycin and penicillin). The cells were maintained in humidified 5% CO_2 incubator, temperature adjusted to 37° C. Cells were maintained for treatment in three different groups, namely (i) Control, (ii) iAs and (iii) iAs+BTE. Cells of the control group were not given BTE or iAs treatment. They were maintained in normal medium, serum and antibiotics. iAs group of cells were maintained in a medium containing 100 nM of Sodium arsenite while the iAs+BTE administered cells were maintained in 100 nM of sodium arsenite and 1 µM of BTE. To mimic chronic iAs exposure, the cells were maintained in respective treatment cultures for a period of 240 days, until clear morphological transformations in the cells were visible.

Estimation of intracellular ROS

2′,7′-dichlorofluorescin diacetate (DCFH-DA) was used to determine ROS. It is cell permeable, oxidation-sensitive and non-polar in nature. ROS was estimated following the standard protocol (Ghosh *et al.,* 2021). DCFH-DA enters the cell and gets converted into DCFH, which is non-fluorescent. Intercellular ROS further oxidises DCFH into fluorescent 2,7-dichlorofluorescein (DCF), which is measured by spectrofluorimeter. In the present study Varian Cary Eclipse spectrofluorimeter was used to record the fluorescent intensity of the excess ROS generated within the cells. 485 nM and 530 nM were the excitation and emission ranges respectively.

Estimation of intracellular Reactive Nitrogen Species (RNS)

RNS generation was measured in the HaCaT cells using the Griess's regent, following the standard protocol (Ghosh *et al.,* 2021). Spectrophotometer was used to record the colorimetric changes, which was used to calculate the amount of RNS generated. Absorbance was measured at 550 nm

Estimation of DNA damage using Micronuclei assay

Micronuclei assay was performed on HaCaT cells after the cells were treated with cytochalasin-B, which stops cytokinesis. The treated cells were then fixed in a fixative (methanol:glacial acetic acid:3:1), were spread on chilled glass slides. They were then stained with stained with 5% Giemsa stained and the number of micronuclei was calculated. Micronuclei was calculated as per 1000 binucleate cells.

Estimation of DNA damage using Single cell Gel electrophoresis (Comet) Assay

Single Cell Gel electrophoresis (SCGE) or comet assay was performed from single cell suspension of HaCaT cells following standard protocols (Sinha *et al.,* 2010).

Estimation of Lipid peroxidation (LPO) assay

HaCaT cells were lysed to extract whole cell proteins, which were then used to perform lipid peroxidation assay. The whole cell proteins were boiled for 1 hour after the addition of 10% SDS, 20% acetic acid, 0.8% thio-barbituric acid (TBA).

After boiling, they were then immediately kept in ice for 10 minutes, which were then subjected to centrifugation at 2500 rpm for 10 minutes. The supernatant was collected and then absorbance of it was measured using spectrophotometer at 535nm. The amount of LPO generated was measured as moles of MDA generated.

Estimation of Protein carbonyl content

Protein carbonyl content in the cell lysates were estimated using Protein Carbonyl Colorimetric Assay Kit by Cayman Chemicals (10005020). Protein carbonyl, in the presence of 2,4-Dinitrophenylhydrazine (DNPH), forms a Schiff's base which can be estimated spectrophotometrically at 360-385 nm.

Estimation of total antioxidant capacity and activity of respective antioxidant enzymes

HaCaT cell lysates were used to measure total antioxidant capacity following the standard protocol mentioned in the Total Antioxidant Assay kit (709001) supplied by Cayman Chemicals. The activity of respective antioxidant enzymes was measured using the standard protocols mentioned in the respective assay kits: Catalase Assay Kit (707002), Superoxide Dismutase Assay Kit (706002), Glutathione Peroxidase Assay Kit (703102), Glutathione Reductase Assay Kit (703202) and Glutathione S-Transferase Assay Kit (703302) all of which were manufactured by Cayman Chemicals.

Estimation of the activity of inflammatory cytokines

Sandwich ELISA technique was used to assess the activity of the pro and anti-inflammatory cytokines. The activities of TNF-α, IL-2, IL-6, CXCL1 IL-8, IL-10, IL-13, IL-17A and IL-22 was measured according to the protocol as mentioned in the respective colorimetric kits TNF alpha ELISA Kit (ab208348), IL-2 ELISA Kit (ab223588), IL-6 ELISA Kit (ab100712), IL-8 ELISA Kit (GRO alpha) (ab213859), IL-10 ELISA Kit (ab255729), IL-13 ELISA Kit (ab219634), IL-17A ELISA Kit (ab199081) and IL-22 ELISA Kit (ab223857), manufactured by Abcam. The reading was taken at 450 nm.

Estimation of activity of NF-κB subunits

The activity of NF-κB p50 and p65 subunits were assessed by the sandwich ELISA technique using NF-κB p50 Transcription Factor Assay Kit (ab207217) and NF-κB p65 ELISA Kit (ab176648) respectively, manufactured by Abcam. The OD was obtained at 450 nm.

Expression of TGF-β and its downstream signalling molecules

The expression of TGF-β and its downstream signalling proteins belonging to both the canonical Smad and noncanonical PI3K-AKT and MAPK pathways have been assessed using Immunoblotting assay. The assay was performed according to the standard protocol (Ghosh *et al.*, 2022b). The bands were scanned and quantified using IMAGE MASTER TM17 2D Elite Software (Amersham Pharmacia biotech Ltd., USA).

Statistical analysis

IBM SPSS Statistics 22 software was used to perform the statistical analysis. One way ANOVA Tukey test was performed to test the significance of the control cells with respect to other treatment cell groups. $p<0.001$ was considered significant while $p<0.0001$ was considered highly significant.

Results and Discussion

Morphological transformation of cells upon iAs treatment and its inhibition by BTE

After 240 days of treatment, prominent morphological transformations were visible in the iAs treated cells. The cells had become elongated, their doubling time had significantly decreased

indicating high proliferation rate and many cells grew on top of one another indicating loss of contact inhibition, all of which suggest carcinogenic transformations within the cell. In the iAs+BTE treated cells, no such morphological transformations were observed and the cells were similar in appearance and proliferation rate as the control cells, even after 240 days of treatment. Results have already been published (Ghosh *et al.*, 2022b)

Generation of free radicles by chronic iAs exposure and its amelioration by BTE

ROS generation in HaCaT cells has been estimated using spectrofluorimeter and has been displayed as a bar graph in Figure 1A. The bar graph clearly indicates that with chronic exposure to iAs there is significant ($p<0.0001$) increase in ROS generation in comparison to the control group of cells. The amount of ROS generated at 240 days in the iAs treated cells is almost double of that observed at 30 days of iAs treatment. In the iAs+BTE treated cells, the ROS generated is significantly ($p<0.0001$) lower than iAs treated cells at 30, 90,150, 210 and 240 days respectively, suggesting that, BTE is able to effectively quench, iAs induced ROS generation, in HaCaT cells. RNS generation has been estimated in the HaCaT cells using spectrophotometer and has been displayed as a bar graph in Figure 1B. RNS generation was measured using Griess' reagent. The obtained results show that, with chronic exposure of iAs there is significant ($p<0.0001$) increase in RNS generation in comparison to the control cells. In the iAs+BTE treated cells, there is significant ($p<0.0001$) quenching of RNS generation with respect to the iAs treated cells, indicating that BTE is able to quench excess RNS generated due to iAs exposure.

Induction of DNA damage upon chronic iAs exposure and its inhibition by BTE

Induction of DNA damage in HaCaT cells has been assessed by Micronuclei assay and Single Cell Gel Electrophoresis (Comet) assay. Figure 2A displays a bar graph showing the number of micronuclei formed per 1000 binucleate cells. According to the bar graph, the number of micronuclei formed is significantly ($p<0.0001$) high in chronically iAs exposed cells than the control cells, suggesting induction of DNA damage by chronic iAs exposure in HaCaT cells. In the iAs+BTE treated cells, the number of micronuclei formed is significantly lower than iAs treated cells implying that BTE prevents iAs induced DNA damage, hence inhibits micronuclei formation in HaCaT cells.

Figure 2B displays a bar graph showing change in comet tail length with respect to increase in treatment time. During electrophoresis, the damaged DNA appears like a comet under the microscope and the length of the tail indicates damaged DNA. From the bar graph it is evident that, at 30 days of iAs treatment itself, there is significant ($p<0.001$) increase in comet tail length in comparison to the control cells. From 90 days onwards, the increase in comet tail length is highly significant ($p<0.0001$) in the iAs exposed cells.

In the iAs+BTE treated cells, the reduction in tail length is significant ($p<0.001$) at 30 days and highly significant ($p<0.0001$) at 90,150,210 and 240 days respectively, in comparison to the iAs treated HaCaT cells. Figure 2C represents a bar graph showing increase in Olive tail moment with respect to treatment time. Olive tail moment is an effective index to measure DNA damage, which is calculated as the product of DNA in the comet tail (%) and corresponding tail length.

The bar graph clearly shows that, with increase in treatment period, there is significant ($p<0.0001$) increase in Olive tail moment, in the iAs treated cells, indicating greater DNA damage. In the iAs+BTE treated cells, the olive tail moment is significantly ($p<0.0001$) low, clearly suggesting that BTE is able to inhibit iAs induced DNA damage. The results of both the micronuclei assay and the comet assay imply that BTE is able to inhibit iAs induced DNA damage in HaCaT cells quite effectively.

Induction of lipid and protein damage by chronic iAs exposure and its mitigation by BTE

Lipid damage was estimated by Lipid Peroxidation assay and the results have been represented as a bar graph in the Figure 3A, where moles of malondialdehyde (MDA) generated has been plotted on the Y axis against treatment time period on the X axis. From the bar graph it can be inferred that, at 30 days of iAs treatment, the moles of MDA generated is significantly ($p<0.001$) higher than the control cells, whereas at 90, 150, 210 and 240 days of treatment, MDA generated in the iAs exposed cells is highly significant ($p<0.0001$), than the control cells, indicating greater lipid damage. In the iAs+BTE treated cells, there is significant ($p<0.001$) reduction in generation of MDA at 30 days, while highly significant ($p<0.0001$) reduction of MDA generation at 90, 150, 210 and 240 days respectively. The result clearly indicates that BTE effectively quenches iAs induced lipid damage in HaCaT cells.

Protein damage has been estimated by protein carbonyl formation assay and the results have been represented as a bar graph in Figure 3B. The graph clearly indicates that at 30 days of iAs exposure, protein carbonyl content is higher than the control cells ($p<0.001$). With further passage of time protein carbonyl content increased; at 90, 150, 210 and 240 days of exposure, the protein carbonyl formation, in the iAs treated cells, is highly significant ($p<0.0001$). This result hints at induction of protein damage due to chronic iAs exposure. In the iAs and BTE treated cells, the reduction of protein carbonyl content is significant ($p<0.001$) at 30, 90,150 days and highly significant ($p<0.0001$) at 210 and 240 days, compared to the iAs exposed cells. The result suggests that BTE effectively mitigates iAs induced lipid and protein damage in HaCaT cells.

Inhibition of the activity of antioxidant enzymes by iAs and its reversal by BTE

Total antioxidative capacity and the activity of specific antioxidant enzymes like Catalase, SOD, GST, GPx and GR have been represented as bar graphs in the Figures 4A, 4B, 4C, 4D, 4E and 4F respectively. From the bar graphs it can be clearly analysed that, with chronic exposure of iAs, there is definitive reduction in total antioxidative capacity, as well as in the activity of respective antioxidant enzymes (Catalase, SOD, GST, GPx, GR) while in the iAs+BTE administered cells, this phenomenon seems to be reversed. The result clearly indicate that chronic exposure to iAs reduces the total antioxidative capacity by inhibiting the activity of respective antioxidative enzymes, which, again appears to be effectively reversed upon BTE treatment.

Induction of inflammation by chronic iAs exposure and its amelioration by BTE

The activity of pro-inflammatory cytokines like TNF-α, IL 2, IL6, IL8, IL13, IL17a, IL22 and anti-inflammatory cytokine IL10 has been represented as a bar-graph in the Figure 5A. The results suggest that, with chronic exposure to iAs, the activity of pro-inflammatory cytokines have significantly ($p<0.0001$) increased with respect to the control cells. The activity of certain pro-inflammatory cytokines like TNF-α, IL17a and IL22 increase to almost three times of that of the control cells, indicating induction of high inflammatory conditions within the cells. The activity of anti-inflammatory cytokine, IL10, reduces significantly ($p<0.0001$) in iAs exposed cells, compared to the control cells hinting at maintenance of chronic inflammatory condition. In the iAs+BTE treated cells, the activity of the pro-inflammatory is significantly ($p<0.0001$) reduced and that of anti-inflammatory cytokine IL10 is significantly ($p<0.0001$) enhanced, compared to the iAs treated cells, displaying inhibition of inflammatory conditions within the cells by BTE.

Figure 5 B displays the bar graph showing the activity of the p50 and p65 subunits of NF-κB, a transcription factor produced due to inflammation. The results clearly point out that with chronic exposure to iAs, there is a significant ($p<0.0001$)

upregulation in the activity of both subunits of NF-κB while in the BTE treated cells, the activity of both subunits (p50 and p65) appear to be significantly ($p<0.0001$) reduced, in comparison to the iAs treated cells. This result clearly suggests that upon chronic iAs exposure, there is induction of chronic inflammatory conditions within the cells, which seem to be effectively quenched upon BTE administration.

Modulation of TGF-β by iAs and its reversal by BTE

Figure 6A shows the representative immunoblot images of TFG-β and its downstream signalling molecules belonging to both canonical (Smad) and non-canonical (PI3K-AKT and MAPK) pathways at 240 days of treatment. The respective immunoblots have been quantified and the band intensities have been represented as bar-graphs in Figure 6B. The results of the Immunoblot assay indicate that, with chronic exposure of iAs, there has been highly significant ($p<0.0001$) upregulation of TGF-β. Downregulation of the expression of Smad 2 and Smad2 was significant ($p<0.001$) and that of Smad 4 was highly significant ($p<0.0001$) in the iAs treated cells with respect to the control, indicating downregulation of the Smad signalling pathway in the iAs treated cells. In the iAs+BTE treated cells too, the reduction in expression of TGF-β was insignificant but the expression of Smad2, Smad 3 and Smad 4 appeared to be significantly ($p<0.001$) and very significantly ($p<0.0001$) upregulated compared to the iAs treated cells. This result suggests that Smad pathway is downregulated upon iAs administration which appears to be reversed upon BTE administration.

The band intensities of the PI3K-AKT pathway suggests that upon chronic iAs exposure, the expression of PI3K, pAKT, p-mTOR, S6K, NF-κBp65 is significantly ($p<0.0001$) upregulated and PTEN is significantly ($p<0.0001$) downregulated, indicating activation of the PI3K-AKT pathway. In the iAs+BTE treated cells, the expression of these signalling intermediates appears to be significantly ($p<0.0001$) reversed suggesting that BTE is downregulating the PI3K-AKT pathway and upregulating PTEN. The downstream signalling molecules of MAPK pathway like pTAK1, pMKK3, pMKK4, p38 and JNK are also significantly ($p<0.0001$) upregulated in the iAs treated HaCaT cells. Upon BTE administration, these MAPK signalling intermediates appear to be significantly ($p<0.0001$) downregulated indicating inhibition of the activity of MAPK pathway in the iAs+BTE treated cells. The obtained results of the immunoblot assay suggests that upon chronic iAs exposure there is increase of expression of TFG-β which conveys its downstream signalling mainly via the non-canonical PI3K-AKT and MAPK pathways whereas in the iAs+BTE treated cells, the expression of TFG-β remains to be unaltered, but propagates its downstream signalling mainly via the canonical Smad pathway.

Normal human skin keratinocytes, HaCaT cells, when chronically exposed to iAs for 240 days, showed prominent morphological transformations. These iAs transformed cells showed hyper proliferative characteristics as well as loss of contact inhibition, suggesting induction of cancer (Ghosh *et al.*, 2022b). The results of the present study imply that, with chronic exposure of iAs, the generation of free radicals in the HaCaT cells increased greatly. Many studies have reported a strong link between chronic induction of free radicals and development of cancer, including skin cancer (Narendhirakannan and Hannah, 2013).

The obtained results also imply that excess ROS generated in iAs exposed HaCaT cells promoted DNA, protein and lipid damage. DNA damage is an established factor leading to carcinogenesis. When DNA damage occurs within tumour suppressor genes or oncogenes and erroneous DNA repair mechanisms fail to repair this damage, it leads to mutations and chromosomal damage within the cells. Accumulation of these damages result in malignant transformations within the cells giving rise to cancer growth (Torgovnick and Schumacher, 2015).

Fig.1 Estimation of free radical generation in Control, iAs and iAs+BTE treated HaCaT cells at different treatment time points. Figure 1 (A) displays a bar graph showing generation of ROS in Control, iAs and iAs+BTE treated HaCaT cells at 30, 90, 150, 210 and 240 days respectively. HaCaT cells were stained with DCFH-DA, ROS generation was measured using a spectrofluorometer and represented as fold change in fluorescent intensity. The increase of ROS generation in the iAs treated cells with respect to the control was significant ($^{a}p<0.0001$) at 30, 90,150,210 and 240 days respectively. The lowering of ROS generation in the iAs+BTE treated cells with respect to iAs exposed cells was significant ($^{x}p<0.0001$) at 30,90,150,210 and 240 days respectively. Figure 1 (B) displays a bar graph showing generation of RNS in the Control, iAs and iAs+BTE treated cells at 30, 90, 150, 210 and 240 days respectively. RNS was estimated using Griess's reagent, recorded using a spectrophotometer and represented as fold change in Nitric Oxide (NO) production. Increase of NO production in the iAs treated cells compared to the Control was significant ($^{a}p<0.0001$) at 30, 90,150,210 and 240 days respectively while lowering of NO production in the iAs+BTE treated cells compared to iAs exposed cells is significant ($^{x}p<0.0001$) at 30,90,150,210 and 240 days respectively. Results are expressed as mean of three independent experiments ± SD.

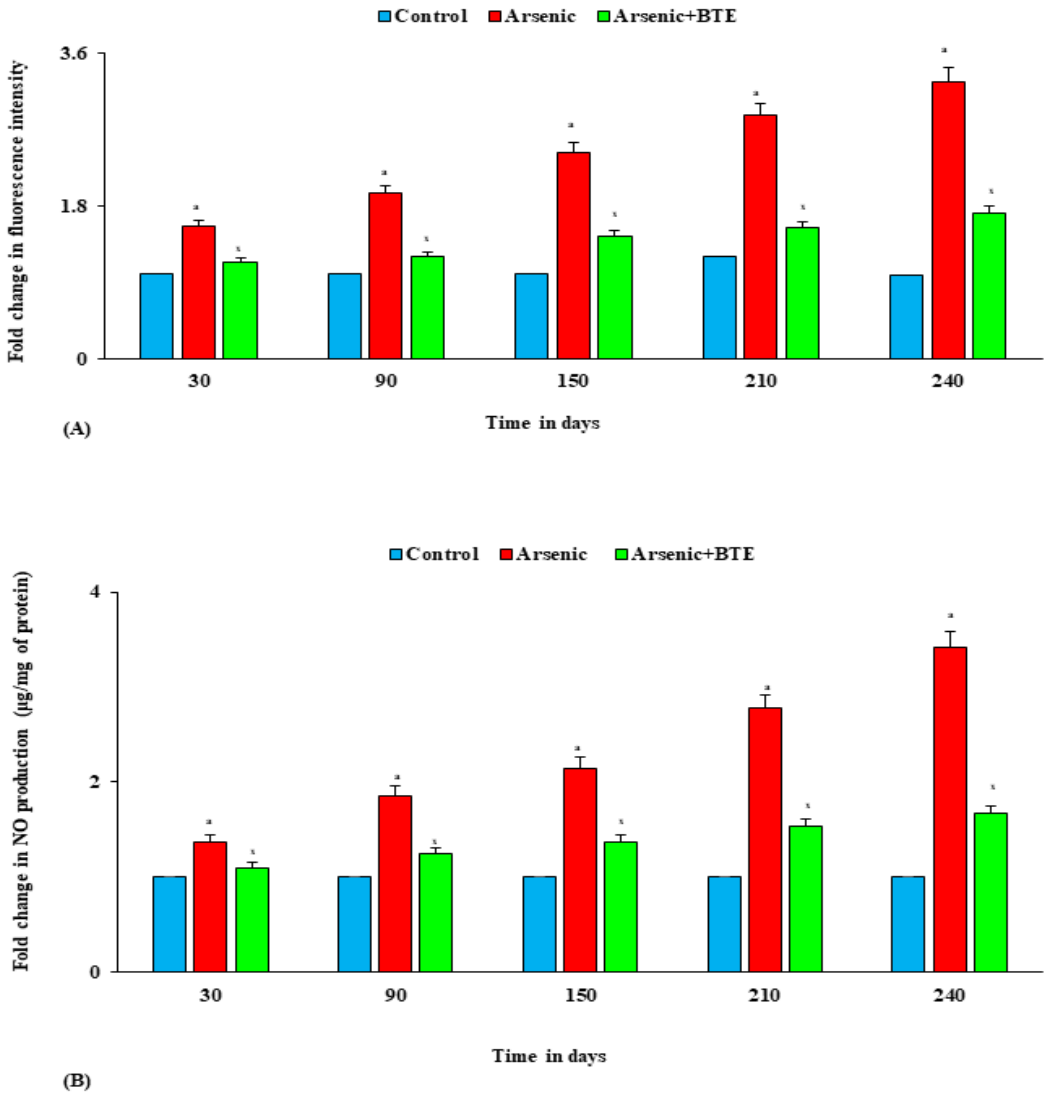

Fig.2 Estimation of DNA damage in Control, iAs and iAs+BTE treated HaCaT cells by Micronuclei Assay and Comet

Assay. Figure 2 (A) displays a bar graph showing number of micronuclei formed per 1000 binucleated cells in Control, iAs and iAs+BTE treated cells at different time points. The cells were fixed and stained with Giemsa. The increase in micronuclei frequency in the iAs treated cells compared to the control was significant ($^{a}p<0.0001$) at 30, 90,150,210 and 240 days respectively. Lowering of the micronuclei frequency in the iAs+BTE treated cells compared to iAs treated cells is significant ($^{x}p<0.0001$) at 30,90,150,210 and 240 days respectively. Figure 2 (B) displays a bar graph showing fold change in comet tail length in Control, iAs and iAs+BTE treated cells at different time points. The DNA of the cells were stained with Ethidium Bromide and observed under fluorescent microscope. The increase in comet tail length in iAs exposed cells compared to control was significant ($^{b}p<0.001$) at 30 days and highly significant ($^{a}p<0.0001$) at 90,150,210 and 240 days respectively. The decrease in tail length in the iAs+BTE treated cells compared to iAs exposed cells was significant ($^{y}p<0.001$) at 30 days and highly significant ($^{x}p<0.0001$) at 90,150,210 and 240 days respectively. Figure 2 (C) displays a bar graph showing fold change in olive tail moment in Control, iAs and iAs+BTE treated cells at different time points. The increase in olive tail moment in iAs exposed cells compared to control was significant ($^{a}p<0.0001$) at 30, 90,150,210 and 240 days respectively. The decrease in tail length in the iAs+BTE treated cells compared to iAs exposed cells was significant ($^{x}p<0.0001$) at 30,90,150,210 and 240 days respectively. Results are expressed as mean of three independent experiments ± SD.

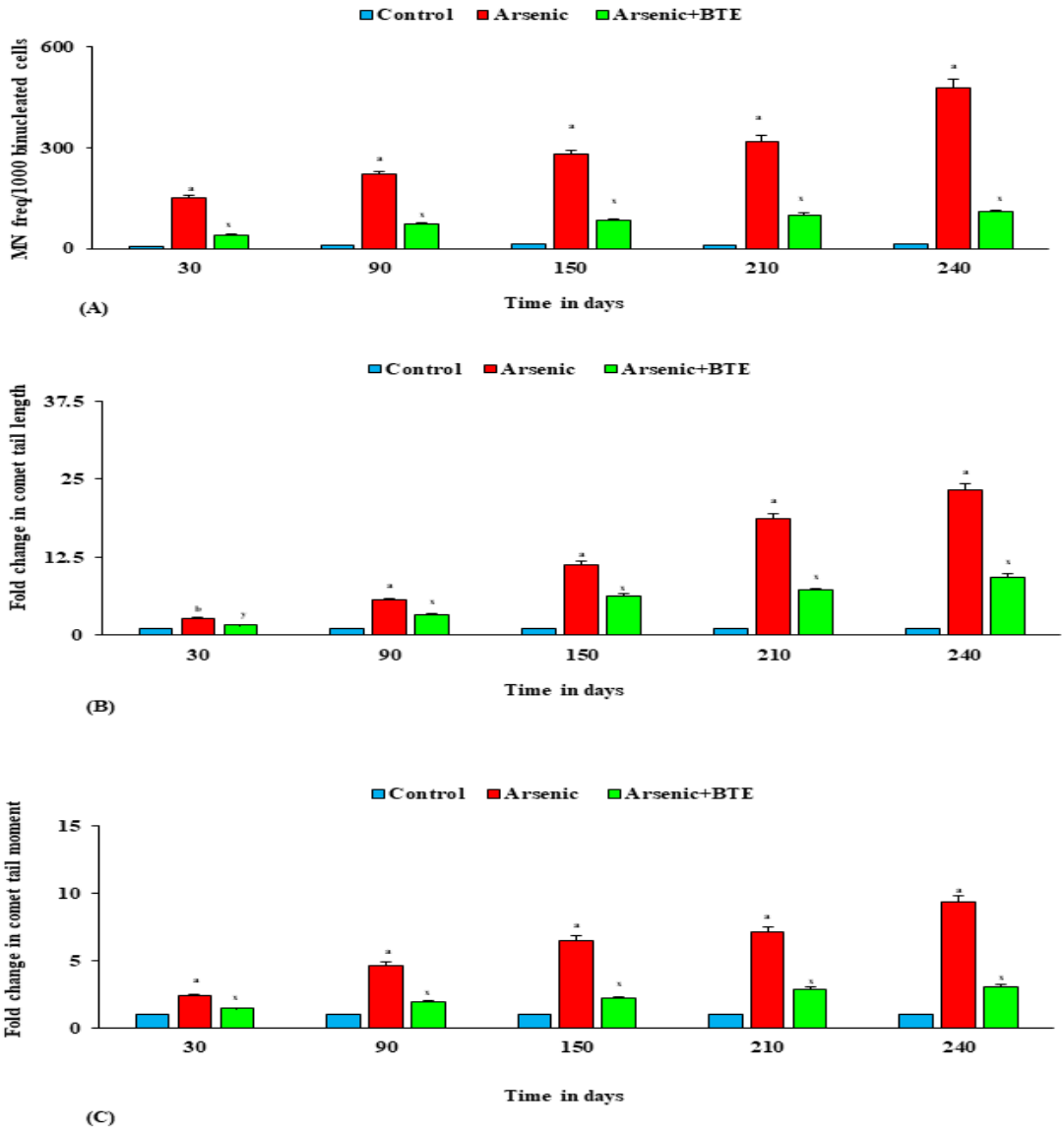

Fig.3 Estimation of Lipid and protein damage in Control, iAs and iAs+BTE treated HaCaT cells by Lipid peroxidation assay and Protein carbonyl assay. Figure 3 (A) displays a bar graph showing moles of MDA generated in Control, iAs and iAs+BTE treated cells at different time points. MDA was estimated using a spectrophotometer. The increase in moles of MDA generated in iAs treated cells compared to the control is significant ($^{b}p<0.001$) at 30 days and highly significant ($^{a}p<0.0001$) at 90,150,210 and 240 days respectively. Lowering of MDA generation in the iAs+BTE treated cells compared to iAs treated cells is significant ($^{y}p<0.001$) at 30 days and highly significant ($^{x}p<0.0001$) at 90,150,210 and 240 days respectively. Figure 3(B) displays a bar graph showing fold change in protein carbonyl content in Control, iAs and iAs+BTE treated cells at different time points. Protein carbonyl formation was estimated using a spectrophotometer. Increase in protein carbonyl content in the iAs treated cells compared to the control was significant ($^{b}p<0.001$) at 30 days and highly significant ($^{a}p<0.0001$) at 90,150,210 and 240 days respectively. The Lowering of protein carbonyl content in the iAs+BTE treated cells compared to iAs treated cells was significant ($^{y}p<0.001$) at 30, 90, 150 days and highly significant ($^{x}p<0.0001$) at 210 and 240 days respectively. Results are expressed as mean of three independent experiments ± SD.

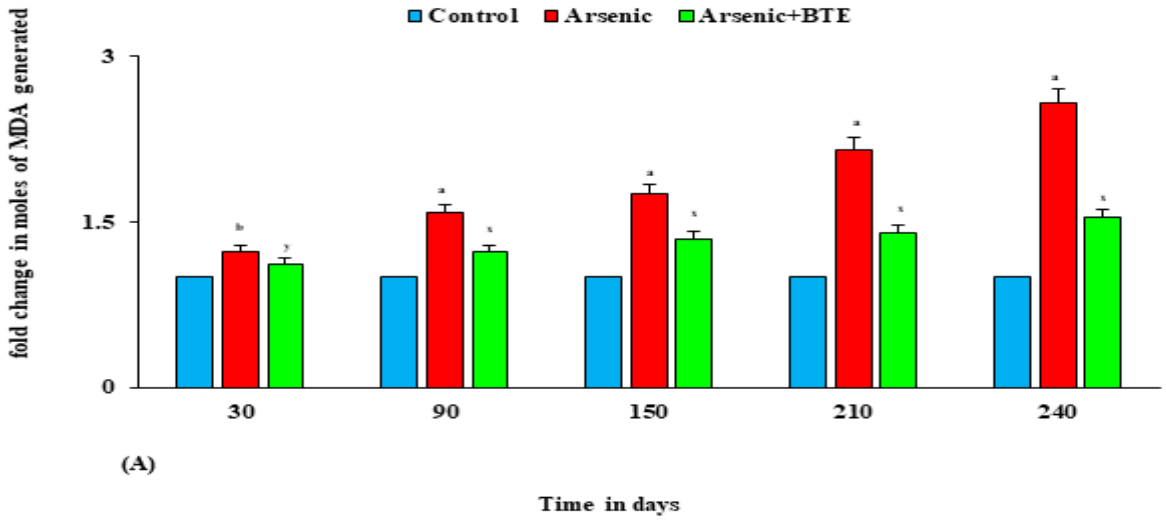

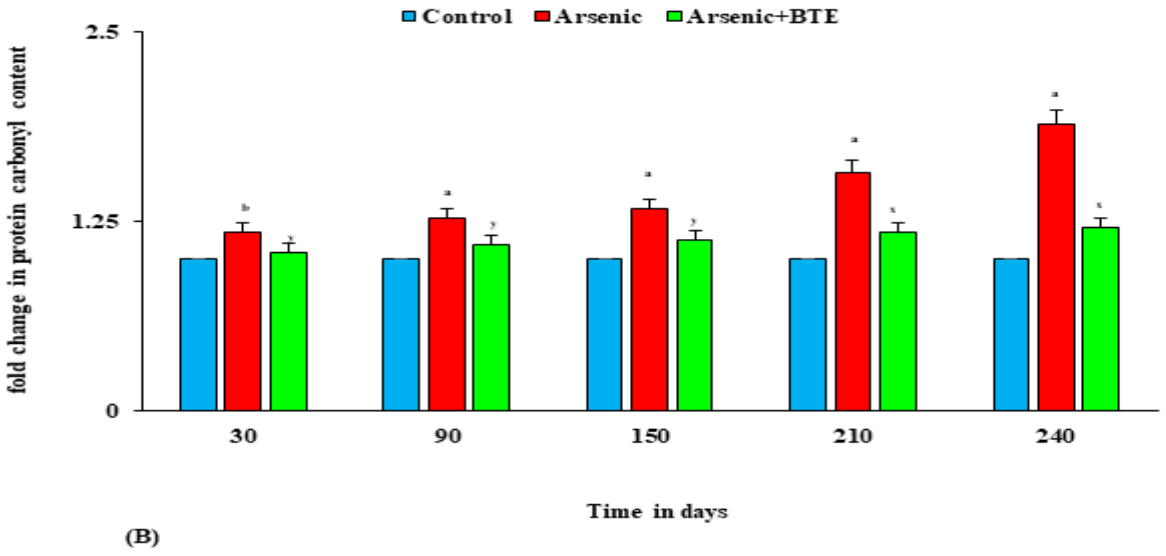

Fig.4 Estimation of Total Antioxidant capacity and antioxidant capacity of the respective antioxidant enzymes in the Control, iAs and iAs+BTE treated HaCaT cells. Figure 4(A) displays a bar graph showing total antioxidant capacity as fold change in Trolox equivalent in Control, iAs and iAs+BTE treated cells at different time points. Figures 4 (B), (C), (D), (E), (F) display bar-graphs showing fold change in Catalase, Super Oxide Dismutase, Glutathione S Transferase, Glutathione Peroxidase and Glutathione Reductase activity respectively. The decrease in antioxidation capacity in the iAs treated cell compared to the control is significant ($^{b}p<0.001$) at 30 days and highly significant at ($^{a}p<0.0001$) at 90, 150, 210 and 240 days respectively. The increase in the antioxidation capacity in the iAs+BTE treated cells compared to the iAs exposed cells is significant ($^{y}p<0.001$) at 30 days and highly significant ($^{x}p<0.0001$) at 90, 150, 210 and 240 days respectively. Results are expressed as mean of three independent experiments ± SD.

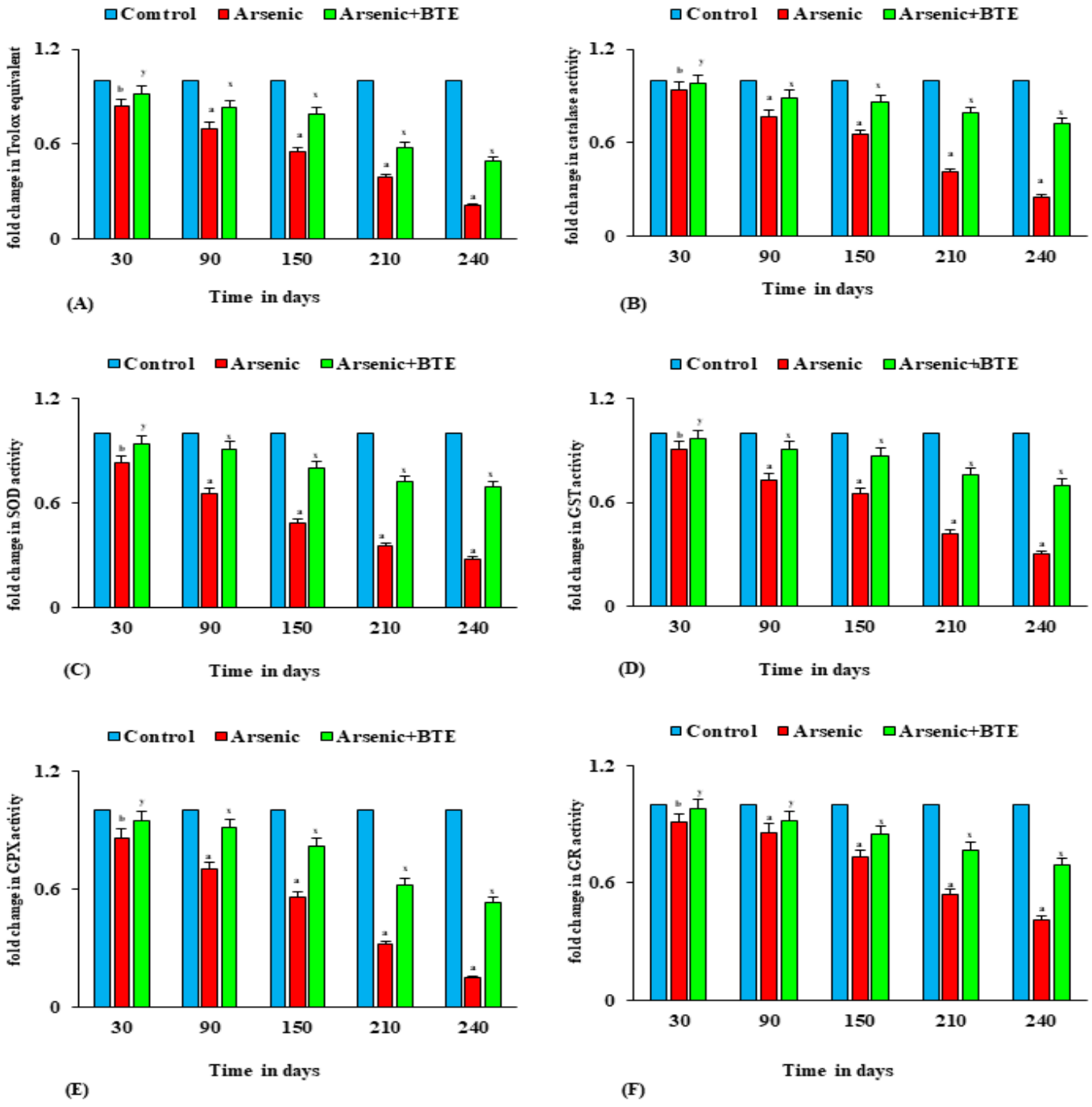

Fig.5 Estimation of the activity of pro-inflammatory and anti-inflammatory cytokine as well as of the p50 and p65 subunits of NF-κB. Figure 5 (A) displays a bar graph showing the activity of pro-inflammatory cytokines TNF-α, IL-2, IL-6, IL-8, IL-13, IL-17a, IL-22 and anti-inflammatory cytokine IL-10 at 30, 150 and 240 days of treatment in Control, iAs and iAs+BTE treated cells. Increase in the activity of pro-inflammatory cytokines and lowering of the activity of anti-inflammatory cytokine (IL-10), in iAs exposed cells, compared to the control is significant ($^{a}p<0.0001$) at 30, 150 and 240 days respectively. Lowering of the activity of pro-inflammatory cytokines and increase in the activity of anti-inflammatory cytokine, in the iAs+BTE administered cells, compared to the iAs exposed cells, is significant ($^{x}p<0.0001$) at 30, 150 and 240 days respectively. The displayed results are mean of three independent experiments ± SD. Figure 5(B) displays a bar graph showing activity of p50 and p65 subunits of NF-κB in the Control, iAs and iAs+BTE treated cells at 30, 150 and 240 days of exposure. The increase in activity of p50 and p65, in iAs exposed cells, compared to control, is significant ($^{a}p<0.0001$) at 30, 150 and 240 days respectively. Decrease in the activity of p50 and p65, in iAs+BTE treated cells, compared to Control, is significant ($^{x}p<0.0001$) at 30, 150 and 240 days respectively. Results are expressed as mean of three independent experiments ± SD.

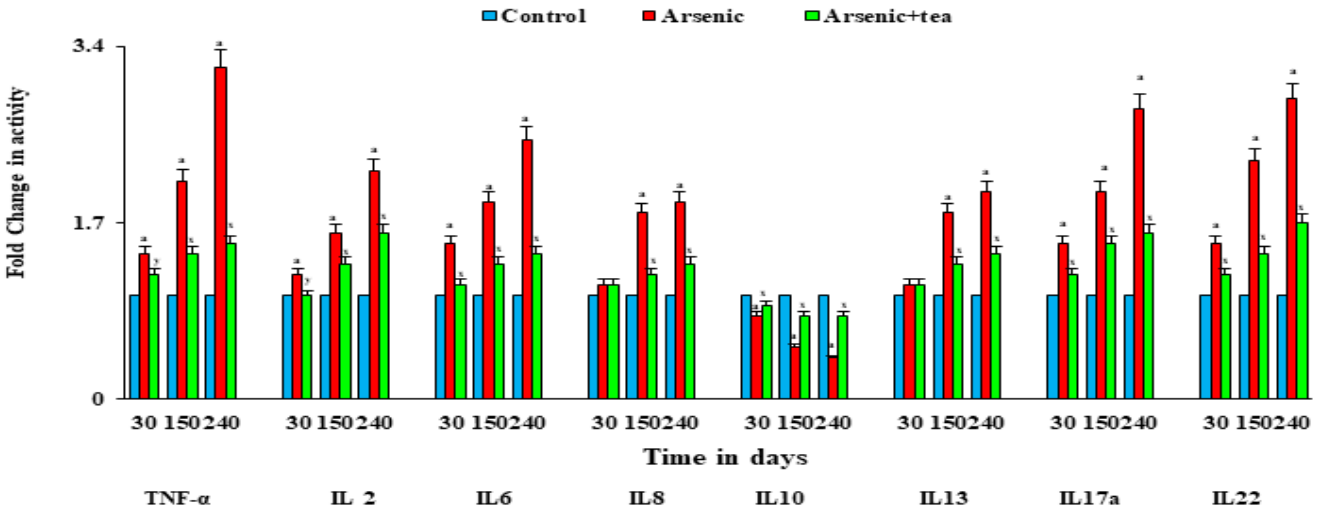

(A)

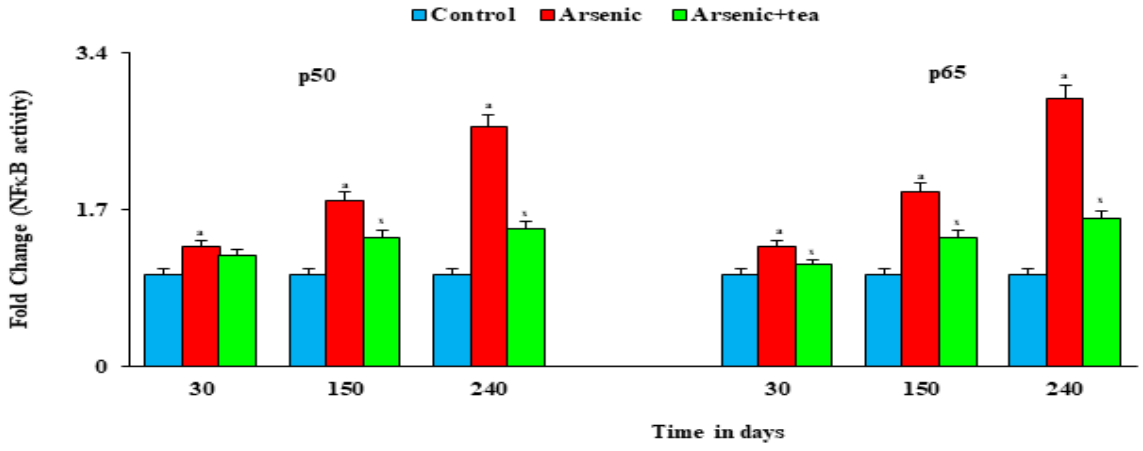

(B)

Fig.6 Investigation of the expression TGF-β and its signalling intermediates of canonical (Smad) and non-canonical (PI3K-AKT and MAPK) pathways, in Control, iAs and iAs+BTE treated HaCaT cells, by Immunoblotting, after 240 days of exposure. Figure 6(A) displays representative immunoblot bands of TGF-β and its downstream signalling proteins, belonging to Smad, PI3K-AKT and MAPK pathways respectively. The lanes 1, 2 and 3 represent control, iAs and iAs+BTE treated HaCaT cells respectively. Figure 6(B) displays a bar graph showing fold change in mean band intensities of TGF-β and its downstream signalling proteins. Modulation of TGF-β expression and its downstream signalling proteins in the iAs treated cells, in comparison to the control cells, is significant at ($^{b}p<0.001$) and highly significant ($^{a}p<0.0001$) at respective time points. Alteration in expression of TGF-β and its downstream signalling proteins, in the iAs+BTE treated cells, in comparison to the iAs exposed cells, is significant ($^{y}p<0.001$) and highly significant ($^{x}p<0.0001$) at respective time points of treatment. Results are expressed as mean of three independent experiments ± SD.

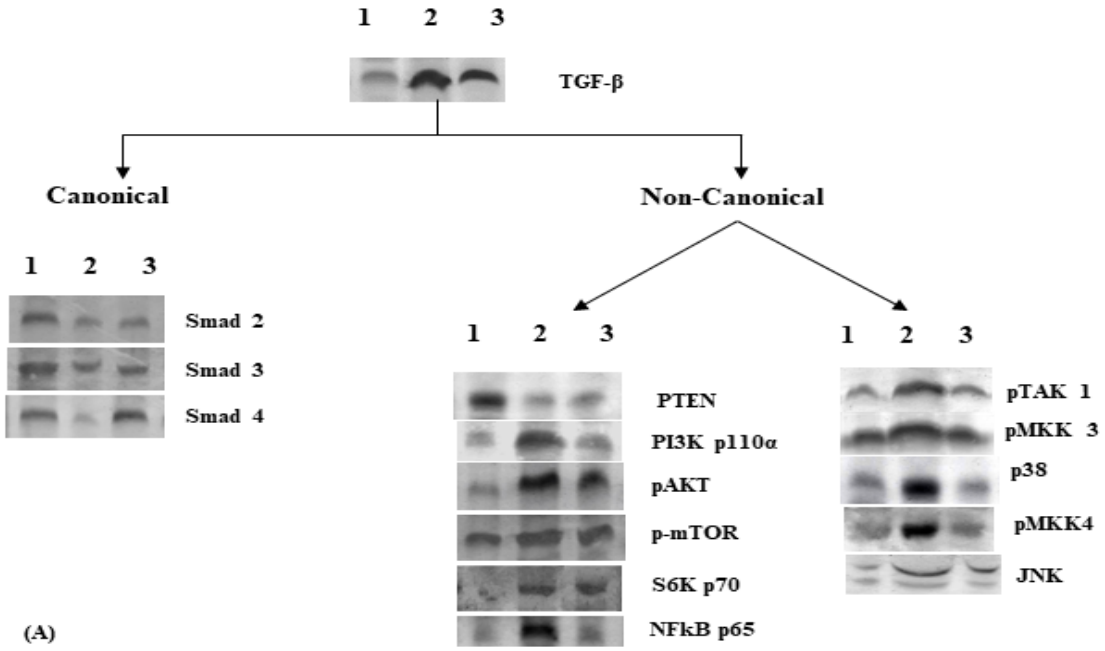

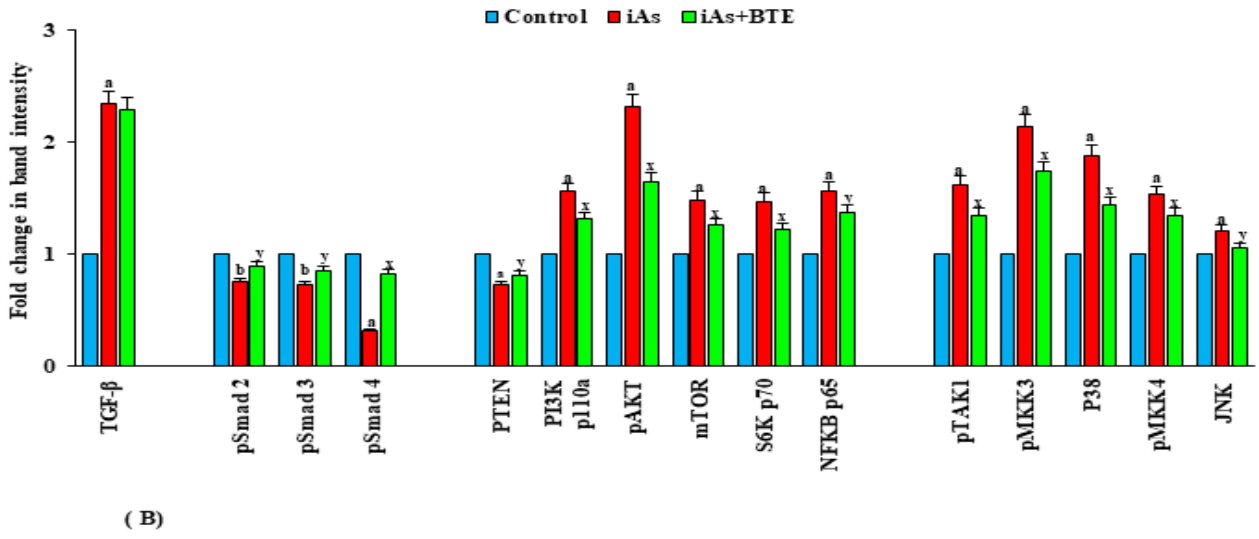

Increase Lipid peroxidation and protein carbonyl content have been found to be directly linked to ROS generation and progression of cancer (Ma *et al.,* 2013), therefore, they are considered to be biomarkers of many diseases, including cancer (Rodríguez-García *et al.,* 2020). Remarkable amplification of DNA damage, elevation of protein carbonylation and lipid peroxidation, in iAs exposed HaCaT cells, in the present study, may strongly indicate towards induction of cancer.

The present study also reports loss of activity of antioxidant enzymes upon chronic iAs exposure. Suppression of activity of antioxidant enzymes upon chronic iAs exposure has also been reported from study on Swiss albino mice (Ghosh *et al.,* 2021). Impaired activity of antioxidant enzymes results in accumulation of unquenched ROS which adds on to the load of free radicals generated by chronic iAs exposure. BTE administered HaCaT cells did not show malignant morphological transformations, as observed in iAs administered cells, highlighting its anti-proliferative property (Ghosh *et al.,* 2022b). Intervention by BTE resulted in quenching of excess ROS, reduction in DNA, protein, lipid damage as well as elevation of activity of antioxidant enzymes in the HaCaT cells, showcasing its ameliorative and chemopreventive property.

Chronic inflammatory conditions are intricately linked to development and progress of cancer (Maru *et al.,* 2014). Prolonged irritation and deregulated inflammation are established skin cancer causing factors. In UV and chemical induced animal models of skin cancer, deregulated and prolonged inflammation plays a pivotal role (Kim *et al.,* 2013). In the present study, the activity of pro-inflammatory cytokines like TNF-α, IL2, IL6, IL8, IL13, IL17a and IL22 were prominently elevated while that of anti-inflammatory cytokine like IL-10 was supressed, in iAs exposed HaCaT cells, indicating induction of chronic inflammatory conditions. Excess ROS generation due to chronic administration of iAs, in Swiss albino mice, has been reported to induce upregulation of pro-inflammatory cytokines and suppression of anti-inflammatory cytokines (Ghosh *et al.,* 2021). BTE, on the other hand, has shown explicit role in supressing the activity of pro-inflammatory cytokines and enhancing the activity of anti-inflammatory cytokine, highlighting its role as an anti-inflammatory agent.

TGF-β is an important cytokine which controls many pathways involved in cell growth and proliferation (Kubiczkova *et al.,* 2012). Elevated levels of TGF-β have been observed in oesophageal, breast, lung, colorectal, pancreatic and gastric cancers (Huang and Blobe, 2016). Upregulation of TGF-β appears to be intricately associated with greater invasiveness, metastasis and poor prognosis (Seoane *et al.,* 2017). Studies have reported that TGF-β is secreted by both the tumour cells as well as by the surrounding stromal cells which help in maintaining the tumour microenvironment (Wever *et al.,* 2008).

TGF-β has also been reported to promote degradation of the extracellular matrix by promoting secretion of matrix metalloproteases, promoting tumour cell invasion. TGF-β has shown prominent role in induction of angiogenesis, EMT, alteration of extracellular matrix and downregulation of immune surveillance (Huang and Blobe, 2016). The results of the present study show that expression of TGF-β is very high in the iAs exposed cells and administration of BTE fails to significantly modulate it. Immunoblots of downstream signalling molecules of TGF-β revealed that, upon chronic iAs exposure, Smad signalling pathway was downregulated, while non-canonical PI3K-AKT and MAPK pathways were upregulated. This phenomenon was found to be reversed upon BTE administration. In the iAs+BTE treated HaCaT cells, the expression of Smad 2, Smad 3 and Smad 4 was found to be effectively higher than in the iAs treated cells. Downregulation of Smad 2, Smad 3 and loss of function of Smad 4 have been reported in a number of cancers, so these Smad molecules may be considered as tumour suppressors (Rose *et al.,* 2018; Hernandez *et al.,* 2019). Upregulation of these proteins by BTE hints at its chemopreventive potential. Upregulation and activation of PI3K, AKT and mTOR is associated with tumour progression

and induction of EMT (Xu *et al.,* 2015). Phosphorylated AKT promotes the activity of mesenchymal factors like Snail and Twist, induces cell motility and invasion by activating S6K as well as stabilises NF-κB (p65) leading to cell proliferation and evasion of apoptosis (Xue *et al.,* 2012; Julien *et al.,* 2007; Acka *et al.,* 2011). Upregulation of the MAPK pathway has also been reported to promote tumour progression. elevation of p38 and JNK has been correlated to induction of EMT (Kudaravalli *et al.,* 2022; Kalli *et al.,* 2022; Zhan *et al.,* 2013). Therefore, upregulation of these non-canonical signalling intermediates of TGF-β pathway, by chronic iAs exposure in HaCaT cells, may promote EMT and ultimately cancer. BTE upregulates tumour suppressor PTEN and effectively downregulates the EMT promoting signalling intermediates of the PI3K-AKT and MAPK pathways, exhibiting its anti-cancer, anti-proliferative potential. Study has reported induction of EMT in HaCaT cells upon chronic iAs exposure (Ghosh *et al.,* 2022b).

The results of the present study clearly indicates that, upon chronic iAs exposure, the upregulated TGF-β acts primarily by the non-canonical PI3K-AKT and MAPK pathways, the signalling intermediates of which have been reported to promote EMT and carcinogenesis. BTE has effectively repressed these EMT promoting signalling intermediates of the PI3K-AKT and MAPK pathways, exhibiting its role in inhibition of iAs induced EMT and cancer. The present study indicates that, BTE can be used as a potential chemopreventive and ameliorative agent against iAs induced excess free radical generation, DNA, lipid, protein damage, compromised antioxidant activity, prolonged inflammation and EMT promoting modulation of TGF-β pathway, all of which may inhibit iAs induced skin cancer.

Acknowledgement

Authors would like to acknowledge Director, Chittaranjan National Cancer Institute (CNCI) for infrastructural facilities and financial support.

References

Akca, H., Demiray, A., Tokgun, O., and Yokota, J. 2011. Invasiveness and anchorage independent growth ability augmented by PTEN inactivation through the PI3K/AKT/NFkB pathway in lung cancer cells. Lung Cancer. 73: 302–309.

Baba, A. B., Rah, B., Bhat, G. R., Mushtaq, I., Parveen, S., Hassan, R., Zargar, M. H., and Afroze, D. 2022. Transforming Growth Factor-Beta (TGF-β) Signaling in Cancer-A Betrayal Within. Front Pharmacol 13:791272.

Boukamp, P., Petrussevska, R. T., Breitkreutz, D., Hornung, J., Markham, A., and Fusenig, N. E. 1988. Normal keratinization in a spontaneously immortalized aneuploid human keratinocyte cell line. J Cell Biol. 106 (3): 761–771.

Chakraborti, D., Singh, S. K., Rahman, M. M., Dutta, R. N., Mukherjee, S. C., Pati, S., and Kar, P. B. 2018. Groundwater Arsenic Contamination in the Ganga River Basin: A Future Health Danger. Int J Environ Res Public Health. 15(2): 180. https://doi.org/10.3390/ijerph15020180

Chung, J. Y., Yu, S. D., and Hong, Y. S. 2014. Environmental source of arsenic exposure. J Prev Med Public Health. 47(5):253–257. https://doi.org/10.3961/jpmph.14.036

Chung, J., Huda, M. N., Shin, Y., Han, S., Akter, S., Kang, I., Ha, J., Choe, W., Choi, T. G., and Kim, S. S. 2021. Correlation between Oxidative Stress and Transforming Growth Factor-Beta in Cancers. Int J Mol Sci. 22 :13181. https://doi.org/10.3390/ijms222413181

Clayton, S. W., Ban, G. I., Liu, C., and Serra, R. 2020. Canonical and noncanonical TGF-β signaling regulate fibrous tissue differentiation in the axial skeleton. Sci Rep. 10 : 21364.

De Wever, O., Demetter, P., Mareel, M., and Bracke, M. 2008. Stromal myofibroblasts are drivers of invasive cancer growth. Int J Cancer. 123(10): 2229–2238. https://doi.org/10.1002/ijc.23925

Ghosh, A., Lahiri, A., Mukherjee, S., Roy, M., and Datta, A. 2022a. Prevention of inorganic arsenic induced squamous cell carcinoma of the skin in Swiss albino mice by black tea

through epigenetic modulation. Heliyon 8: e10341.

Ghosh, A., Mukherjee, A., Mukherjee, S., and Roy, M., 2020. Assessment of Susceptibility towards iAs Induced Carcinogenesis in West Bengal, India. Int J Curr Microbiol App Sci.9(3): 1998-2011. https://doi.org/10.20546/ijcmas.2020.903.232

Ghosh, A., Mukherjee, S., and Roy, M. 2022b. Black tea extract prevents inorganic arsenic induced uncontrolled proliferation, epithelial to mesenchymal transition and induction of metastatic properties in HaCaT keratinocytes - an in vitro study. Toxicol In Vitro. 85:105478. https://doi.org/10.1016/j.tiv.2022.105478

Ghosh, A., Mukherjee, S., and Roy, M., 2021. Chemopreventive role of black tea extract in Swiss albino mice exposed to inorganic arsenic. Asian Pac J Cancer Prev. 22 (11): 3647. https://doi.org/10.31557/APJCP.2021.22.11.3647

Hanahan, D., and Weinberg, R. A. 2011. Hallmarks of cancer: the next generation. Cell. 144(5): 646–674.

Hao. Y., Baker, D., and Ten-Dijke, P. 2019. TGF-β-Mediated Epithelial-Mesenchymal Transition and Cancer Metastasis. Int J Mol Sci. 20(11):2767. https://doi.org/10.3390/ijms20112767

Hernandez, A. L., Young, C. D., Wang, J. H., and Wang, X. J. 2019. Lessons learned from SMAD4 loss in squamous cell carcinomas. Mol Carcinog. 58(9):1648-1655. https://doi.org/10.1002/mc.23049

Huang, J. J., and Blobe, G. C. 2016. Dichotomous roles of TGF-β in human cancer. Biochem Soc Trans. 44(5):1441-1454. https://doi.org/10.1042/BST20160065

Hunt, K. M., Srivastava, R. K., Elmets, C. A., and Athar, M. 2014. The mechanistic basis of arsenicosis: pathogenesis of skin cancer. Cancer Lett. 354(2): 211–219. https://doi.org/10.1016/j.canlet.2014.08.016

Julien, S., Puig, I., Caretti, E., Bonaventure, J., Nelles, L., van Roy, F., Dargemont, C., de Herreros, A. G., Bellacosa, A., and Larue, L. 2007. Activation of NF-kB by Akt upregulates Snail expression and induces epithelium mesenchyme transition. Oncogene 26: 7445–7456. https://doi.org/10.1038/sj.onc.1210546

Kalli, M., Li, R., Mills, G. B., Stylianopoulos, T., and Zervantonakis, I. K. 2022. Mechanical stress signalling in pancreatic cancer cells triggers p38 MAPK- and JNK-dependent cytoskeleton remodelling and promotes cell migration via Rac1/cdc42/Myosin II. Mol Cancer Res. 20 : 485–497. https://doi.org/10.1158/1541-7786.MCR-21-0266

Kim, Y., Lee, S. K., Bae, S., Kim, H., Park, Y., Chu, N. K., Kim, S. G., Kim, H. R., Hwang, Y. I., Kang, J. S., and Lee, W. J. 2013. The anti-inflammatory effect of alloferon on UVB-induced skin inflammation through the down-regulation of pro-inflammatory cytokines. Immunol Lett. 149(1-2): 110–118. https://doi.org/10.1016/j.imlet.2012.09.005

Krstić, J., Trivanović, D., Mojsilović, S., and Santibanez, J. F. 2015. Transforming Growth Factor-Beta and Oxidative Stress Interplay: Implications in Tumorigenesis and Cancer Progression. Oxid Med Cell Longev. 2015: 654594. https://doi.org/10.1155/2015/654594

Kubiczkova, L., Sedlarikova, L., Hajek, R., and Sevcikova, S. 2012. TGF-β - an excellent servant but a bad master. J Transl Med. 10: 183. https://doi.org/10.1186/1479-5876-10-183

Kudaravalli, S., Den Hollander, P., and Mani, S. A. 2022. Role of p38 MAP kinase in cancer stem cells and metastasis. Oncogene 41: 3177–3185. https://doi.org/10.1038/s41388-022-02329-3

Lamouille, S., Xu, J., and Derynck, R. 2014. Molecular mechanisms of epithelial-mesenchymal transition. Nat Rev Mol Cell Biol. 15: 178–196. https://doi.org/10.1038/nrm3758

Lingappan, K. 2018. NF-κB in Oxidative Stress. Curr Opin Toxicol. 7:81-86. https://doi.org/10.1016/j.cotox.2017.11.002

Lu, Q., Wang, W. W., Zhang, M. Z., Ma, Z. X., Qiu, X. R., Shen, M., and Yin, X. X. 2019. ROS induces epithelial-mesenchymal transition via the TGF-β1/PI3K/Akt/mTOR pathway in diabetic nephropathy. Exp Ther Med 17: 835–846. https://doi.org/10.3892/etm.2018.7014

Ma, Y., Zhang, L., Rong, S., Qu, H., Zhang, Y.,

Chang, D., Pan, H., and Wang, W. 2013. Relation between gastric cancer and protein oxidation, DNA damage, and lipid peroxidation. Oxid Med Cell Longev. 543760. https://doi.org/10.1155/2013/543760

Maru, G., Gandhi, K., Ramchandani, A., and Kumar, G. 2014. Inflammation and Cancer. In 'The role of inflammation in skin cancer', Eds. (Aggarwal, B. B., Sung, B., and Gupta, C.). Springer: 437-469. https://doi.org/10.1007/978-3-0348-0837-8_17

Mittal, M., Siddiqui, M. R., Tran, K., Reddy, S. P., Malik, A. B. 2014. Reactive oxygen species in inflammation and tissue injury. Antioxid Redox Signal. 20(7):1126-1167. https://doi.org/10.1089/ars.2012.5149

Narendhirakannan, R. T., and Hannah, M. A. 2013. Oxidative stress and skin cancer: an overview. Indian J Clin Biochem. 28(2):110-115. https://doi.org/10.1007/s12291-012-0278-8

Rahaman, M. S., Rahman, M. M., Mise, N., Sikder, M. T., Ichihara, G., Uddin, M. K., Kurasaki, M., and Ichihara, S. 2021. Environmental arsenic exposure and its contribution to human diseases, toxicity mechanism and management. Environ Pollut. 289: 117940. https://doi.org/10.1016/j.envpol.2021.117940

Ranjan, A., Ramachandran, S., Gupta, N., Kaushik, I., Wright, S., Srivastava, S., Das, H., Srivastava, S., Prasad, S., and Srivastava, S. K. 2019. Role of Phytochemicals in Cancer Prevention. Int J Mol Sci 20: 4981. https://doi.org/10.3390/ijms20204981

Rodríguez-García, A., García-Vicente, R., Morales, M. L., Ortiz-Ruiz, A., Martínez-López, J., and Linares, M. 2020. Protein Carbonylation and Lipid Peroxidation in Hematological Malignancies. Antioxidants. 9(12):1212. https://doi.org/10.3390/antiox9121212

Rose, A. M., Spender, L. C., Stephen, C., Mitchell, A., Rickaby, W., Bray, S., Evans, A. T., Dayal, J., Purdie, K. J., Harwood, C. A., Proby, C. M., Leigh, I. M., Coates, P. J., and Inman, G. J. 2018. Reduced SMAD2/3 activation independently predicts increased depth of human cutaneous squamous cell carcinoma. Oncotarget 9:14552–14566. https://doi.org/10.18632/oncotarget.24545

Roy, M., Mukherjee, A., Mukherjee, S., and Biswas, J. 2014. Arsenic: an alarming global concern. Int J Curr Microbiol App Sci. 3(10): 34-47

Seoane, J., and Gomis, R. R. 2017. TGF-β Family Signaling in Tumor Suppression and Cancer Progression. Cold Spring Harb Perspect Biol. 9(12): a022277. https://doi.org/10.1101/cshperspect.a022277

Sinha, D., Roy, S., and Roy, M. 2010. Antioxidant potential of tea reduces arsenite induced oxidative stress in Swiss albino mice. Food Chem Toxicol. 48: 1032–1039. https://doi.org/10.1016/j.fct.2010.01.016

Srinivas, U. S., Tan, B. W. Q., Vellayappan, B. A., and Jeyasekharan, A. D. 2019. ROS and the DNA damage response in cancer. Redox Biol. 25: 101084. https://doi.org/10.1016/j.redox.2018.101084

Torgovnick, A., and Schumacher, B. 2015. DNA repair mechanisms in cancer development and therapy. Front Genet. 6:157. https://doi.org/10.3389/fgene.2015.00157

Vincent, T., Neve, E. P. A., Johnson, J. R., Kukalev, A., Rojo, F., Albanell, J., Pietras, K., Virtanen, I., Philipson, L., Leopold, P. L., Crystal, R. G., de Herreros, A. G., Moustakas, A., Pettersson, R. F., and Fuxe, J. 2009. A SNAIL1-SMAD3/4 Transcriptional Repressor Complex Promotes TGF-Beta Mediated Epithelial-Mesenchymal Transition. Nat Cell Biol. 11 : 943–950. https://doi.org/10.1038/ncb1905

Xu, W., Yang, Z., and Lu, N. 2015. A new role for the PI3K/Akt signalling pathway in the epithelial-mesenchymal transition. Cell Adh Migr. 9(4): 317-324. https://doi.org/10.1080/19336918.2015.1016686

Xue, G., Restuccia, D. F., Lan, Q., Hynx, D., Dirnhofer, S., Hess, D., Rüegg, C., and Hemmings, B. A. 2012. Akt/PKB-mediated phosphorylation of Twist1 promotes tumor metastasis via mediating cross-talk between PI3K/Akt and TGF-b signaling axes. Cancer Discov. 2 : 248–259. https://doi.org/10.1158/2159-8290.CD-11-0270

Yusupov, M., Wende, K., Kupsch, S., Neyts, E. C., Reuter, S., and Bogaerts, A. 2017. Effect of head group and lipid tail oxidation in the cell membrane revealed through integrated

simulations and experiments. Sci Rep. 7(1): 5761. https://doi.org/10.1038/s41598-017-06412-8

Zhan, X., Feng, X., Kong, Y., Chen, Y., and Tan, W. 2013. JNK signaling maintains the mesenchymal properties of multi-drug resistant human epidermoid carcinoma KB cells through snail and twist1. BMC cancer 13: 180. https://doi.org/10.1186/1471-2407-13-180

Zhang, Y. 2009. Non-Smad pathways in TGF-β signaling. Cell Res. 19: 128–139. https://doi.org/10.1038/cr.2008.328

How to cite this article:

Archismaan Ghosh and Madhumita Roy. 2023. Black Tea Extract Prevents iAs Induced Transformation of HaCaT Cells via Modulation of Cellular Damage, Inflammation and TGF-β Signalling Cascade. *Int.J.Curr.Microbiol.App.Sci.* 12(01): 171-189. **doi:** https://doi.org/10.20546/ijcmas.2023.1201.020